Nigerian Research Journal of Chemical Sciences **(ISSN: 2682-6054)**
Volume 11, Issue 2, 2023

Removal of Rhodamine B Dye from Aqueous Solution Using Copper(II) Oxide/Cellulose Acetate Nanocomposite

[*1]Nwosu, F.O., [2]Abdullahi, M. R., [1]Adebayo, G.B., [1]Jesekunle, D. O. and [3]Dikwa, M. K.

[1]Department of Industrial Chemistry, Faculty of Physical Sciences, University of Ilorin, Ilorin, Nigeria

[2]Department of Pure and Industrial Chemistry, Faculty of Physical Sciences, Bayero University, Kano, Nigeria

[3] Department of Pure and Applied Chemistry, University of Maiduguri

*Corresponding Author: f.o.nwosu@gmail.com

ABSTRACT

In this work, the adsorptive performance of adsorbent derived from copper oxide cellulose acetate, CuO/CA nanocomposite was investigated for the removal of Rhodamine B dye from aqueous solution. The copper oxide nanoparticle was prepared by coprecipitation method using copper chloride and sodium hydroxide while the nanocomposite was obtained from mixture of copper oxide nanoparticles and cellulose acetate in the presence of hydrochloric acid. The prepared CuO/CA nanocomposite adsorbents was characterized by using scanning electron microscope coupled with energy dispersive x-ray (SEM-EDX), Brunauer-emette-teller (BET) method and Fourier transform infrared (FTIR). The BET surface area was 275.68 m^2/g. The adsorption of Rhodamine B dye onto nanocomposite was dependent on the initial dye concentration, contact time, adsorbent dose, temperature and the maximum adsorption capacity was reached at 50 mg/L, contact time of 180 minutes and adsorbent dosage of 0.1 g. The adsorption isotherm and kinetic studies were best described by Langmuir isotherm model and pseudo second-order kinetic model with correlation coefficients, R^2 of 0.920 and 0.968 respectively. The value of separation factor, R_L was 0.09 indicating a favourable adsorption process. The result of thermodynamic parameters revealed feasible, spontaneous and endothermic process with increase in randomness at the interface. The study concluded that CuO/CA was effective in the removal of Rhodamine B dye from aqueous solution.

Keywords: Adsorption, cellulose acetate, CuO, nanocomposite, Rhodamine B

INTRODUCTION

Textile industries are the largest consumer of synthetic dyes utilizing about 56% of the total world dyes production per annum [1]. The effluents from textile dyeing industries are mostly

released into water body without any treatment and this caused severe threats to aquatic organisms and the entire environment [2]. The physical and chemical properties of water such as colour, taste, odour, alkalinity, and acidity are greatly affected due to the presence of dyes. They affect the overall quality of water making it unsuitable for domestic and commercial purposes. Dyes are not biodegradable, possess complex aromatic structure and are toxic even at low concentration as they cause cancer and may damage some vital organs in human beings, such as dysfunction of the kidneys, reproductive system, liver, brain and central nervous system [3].

Different treatment methods such as adsorption, precipitation [4] ion-exchange, and reverse osmosis [5] have been employed for the removal of dyes from aqueous solution. However, the process of adsorption has been widely used as effective method for a wide range of dissolved pollutants from aqueous solution due to its efficiency, low cost and easy operation [6, 7]. Adsorbent derived from ZnO/Ac nanocomposites was used for the removal of methylene blue dye from aqueous solution. The maximum percentage removal was 92% at pH 10, concentration of 50 mg/L, contact time of 150 min and adsorbent dosage of 50 mg [8]. Adsorption performance of adsorbent produced from Fe_3O_4-CuO-activated carbon nanocomposites was investigated for the removal of bromophenol blue dye from aqueous solution. It was found that that the maximum removal efficiency achieved was 97% at pH 9 and adsorbent dosage of 0.06 g/L [9]. Agricultural waste obtained from *Raphia hookerie* fruit epicarp was used as adsorbent for the removal of Rhodamine B dye from aqueous solution and it was found that the maximum adsorption capacity achieved at 400 mg/L was 312 mg/g [10].

In the present study, adsorbent derived from copper(II) oxide/cellulose acetate (CuO/CA) nanocomposite was used for the removal of Rhodamine B dye from aqueous. Adsorption isotherms, kinetics and thermodynamics were also investigated.

MATERIALS AND METHODS

The chemical used in this study were of analytical grade. These include: copper(II) chloride, $CuCl_2 \cdot 2H_2O$, sodium hydroxide, NaOH (park scientific, purity, 97%), hydrochloric acid, HCl (specific gravity, 1.18 purity, 36%), de-ionized water and acetic acid. The apparatus used in the study were beakers, standard volumetric flasks, micropipette, round bottom flasks, glass wares and other general appatatus required in a chemical laboratory. The instruments that were used include pH metre (HI 9813-6), water bath shaker (WHY-2 model), muffle furnace (carbolite ELF 11/1AB) and spectroscopic instruments like FTIR, SEM-EDX, BET and UV- Visible.

Sample Preparation

Preparation of copper(II) oxide (CuO) nanoparticles

Copper oxide (CuO) nanoparticles were prepared as reported by Rahdar *et al*. [11] using $CuCl_2.4H_2O$ and NaOH as the precipitating agent. About 1.7 g of $CuCl_2.4H_2O$ was dissolved in 50 mL de-ionized water and the solution was magnetically stirred at 50 °C for 40 minutes, then 0.1M NaOH solution was added to adjust the pH to 10. The colour changed from pale blue to dark blue after addition of NaOH. The blue precipitates that were formed were then filtered, washed with de-ionized water and 50 mL ethanol and then finally dried in an oven at 60 °C for 4 hours. The dried sample was then calcined at 400 °C for 2 hours to obtain CuO nanoparticles. During calcinations the colour of the sample changed from dark blue to black [11].

Preparation of Cellulose Acetate from Agricultural Waste

About 50.0 g of ground sugar cane bagasse was washed to remove impurities. The residue was dried under room temperature and later suspended in 18% NaOH and heated for 2 hours to remove hemicelluloses. The mixture was filtered and the residue was washed until it was no longer soapy and free of NaOH. The 80 mL solution of glacial acetic acid was added to the residue, and heated under water bath for 2 hours. The pure white cellulose obtained was washed, dried and kept in air tight container. About 25 g of the prepared cellulose was soaked in 100 mL of glacial acetic acid. The solution was kept in water bath at 55 ^oC for 1 hour with frequent stirring. Acetylation was carried out by mixing 0.8 mL of conc. H_2SO_4 and 50 mL of acetic anhydride upon frequent stirring at 55 ^oC till colloidal solution was obtained and then filtered [12].

Preparation of nanocomposite

The composite of copper oxide/cellulose acetate was prepared according to the method reported by Tahir *et al* [12]. This was done in 1:1 ratio in which the mixture of CuO/Cellulose acetate was dispersed in 0.5 M HCl to form a colloidal solution. The solution was stirred and evaporated to dryness in an oven. The composite material was washed with de-ionized water, filtered and further dried in an oven at 100 ^oC for 12 hours and kept in a container for further use.

Adsorption Studies

Effect of initial concentration

About 25 mL of Rhodamine B dye solution with concentrations ranging from 5-70 mg/L was placed in each conical flask and contacted with 0.1 g of adsorbent for 4 hours at room temperature in a water bath shaker. After that, the solutions were filtered and absorbance of the solutions was measured using UV-visible spectrophotometer (Jenway 7300 spectrophotometer) [13].

Effect of contact time

About 25 mL of Rhodamine B dye solution at optimum concentration was transferred into conical flasks and contacted with 0.1 g of adsorbent at varying time from 5 to 180 minutes in a water bath shaker at room temperature. The solutions were filtered and the absorbances of the filtrates were measured using Uv-visible spectrophotometer [14].

Effect of Adsorbent Dosage

About 25 mL of Rhodamine B dye solution at optimum conditions was transferred into different conical flasks. The solutions were contacted with varying amount of adsorbent ranging from 0.1-0.5 g in a water bath shaker. The solutions were filtered and the absorbance of the residual filtrates was measured using Uv-visible spectrophotometer [14].

Effect of Temperature

About 25 mL of Rhodamine B dye solution at optimum conditions was transferred into different conical flasks. The temperature of the solutions were varied between 30 ^{0}C to 70 ^{0}C and placed in a water bath shaker. The solutions were filtered. The residual filtrates were measured using Uv-visible spectrophotometer [14].

The adsorption capacity of Rhodamine B dye onto CuO/CA nanocomposite was calculated using Eq. 1:

$$Qe = \frac{(C_0 - Ce\ )V}{M} \qquad (1)$$

Where Qe (mg/g) is the adsorption capacity, C_0 (mg/L) is the initial concentration of dye in the solution, Ce (mg/L) is equilibrium concentration of dye in the solution, V (L) is the volume of the solution used in the flask and M (g) is the amount of nanocomposite adsorbent used .

Instrumental characterization

The surface functional groups of the adsorbent were detected using Fourier Transform Infrared, FTIR spectrometer (Nicolet IS10 FTIR spectrometer). The specific surface areas and pore volumes were determined by Brunauer–Emmet–Teller (BET) method using nitrogen adsorption at 77K by using automated surface area analyzer (JW-DA 76502057en) while the surface morphology and elemental compositions were determined using scanning electron microscopy (SEM) coupled with EDX (JOEL-JSM-7600F).

RESULTS AND DISCUSSION

Characterization of the Adsorbent

BET analysis

Table 1 presents the results of single point BET analysis of the surface area and that of BJH method for pore volume and pore size respectively.

Table 1: surface are and porosity measurement of CuO/CA nanocomposites

Adsorbent	BET surface area (m^2/g)	Pore volume (cm^3/g)	Pore size (nm)
CuO/CA nanocomposite	275.68	0.66	3.03

The result of BET surface area and porosity measurement of CuO/CA nanocomposite is presented in Table 1. The surface area is an important factor that is indicating the applicability of adsorbent for heavy metal or dye removal from aqueous solution [15]. The surface area of the nanocomposite was 275.68 m^2/g and is higher than the reported value of 51.1 m^2/g obtained using different composites [16], while its pore volume and pore size were 0.66 cm^3/g and 30.3 nm respectively. According to IUPAC, pore sizes have been classified into micropore (1-2 nm), mesopore (2-50 nm) and macropores (greater than 50 nm). It could be observed that the value obtained lies between 2–50 nm indicating that CuO/CA nanocomposite is mesoporous in nature [17].

FTIR analysis

The result of FTIR analysis of CuO/CA nanocomposite is shown in Fig. 1. The FTIR analysis showed a presence of broad absorption at 3479.00 cm^{-1} which could be due to O-H stretching vibration. The sharp peak at 1641.52 cm^{-1} may be attributed to C=O of the carbonyl group. A similar observation has been reported [13] while the absorption peak around 456.00 cm^{-1} could be due to metal oxygen bond [11].

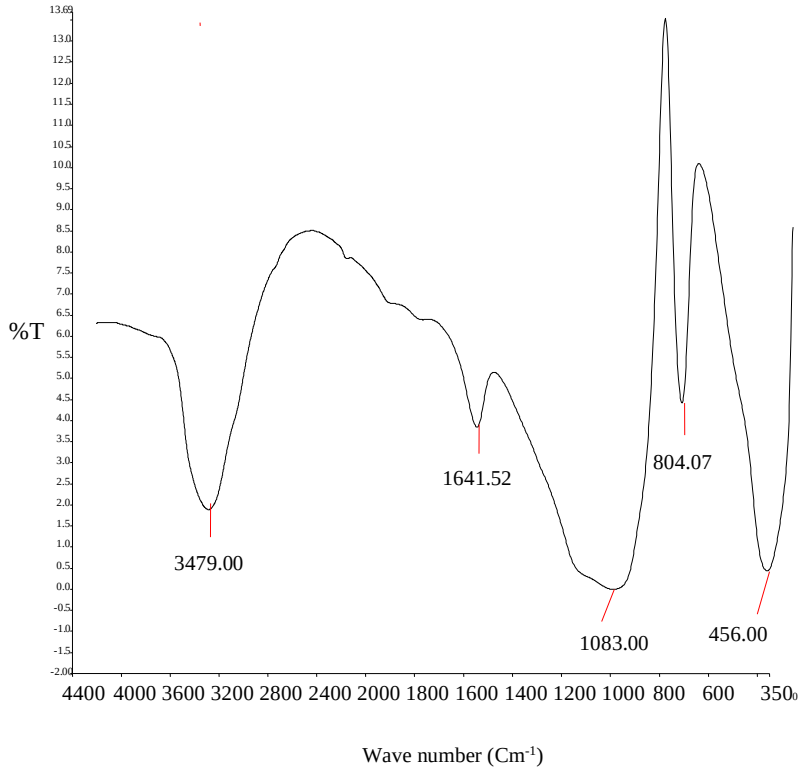

Fig 1: FTIR spectrum of CuO/CA nanocomposite

SEM/EDX analysis

The results of SEM/EDX analysis of CuO/CA nanocomposite are shown in Figs. 2 and 3. The SEM micrograph of CuO/CA nanocomposite as shown in Fig. 2 revealed the presence of rough surface area which is generally believed to be a requirement for adsorptive properties of a good adsorbent. It is generally observed that pore structure development is influenced by many factors, such as inorganic impurities and the initial structure of the carbon precursor [18]. The elemental composition of CuO/CA nanocomposite as presented in Fig. 3 revealed that copper and oxygen are the major element which indicates that CuO nanoparticles has been successfully

prepared while the presence of some element such as lead in small quantity might have been originated from the precursor used or during manufacturing processes.

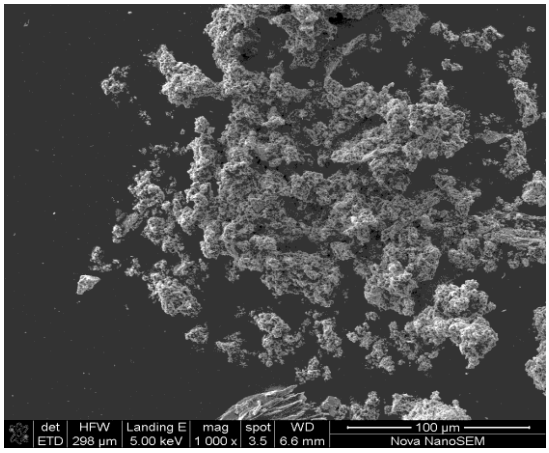

Fig. 2: SEM micrograph of CuO/CA nanocomposite at magnification of x1000

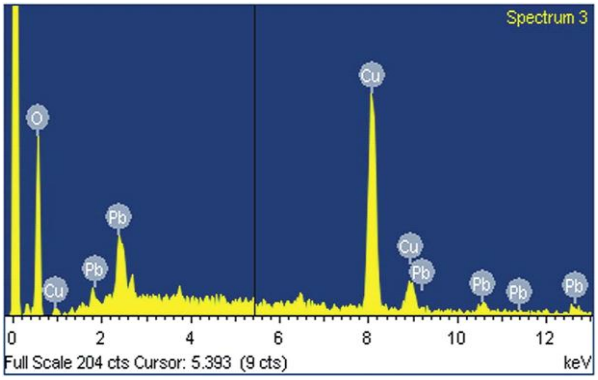

Fig. 3: EDX spectrum of CuO/CA nanocomposite

Batch adsorption studies

Effect of initial dye concentration

The result of effect of initial concentration for the uptake of Rhodamine B dye onto CuO/CA nanocomposite is shown in Fig. 4. It could be observed that increase in initial dye concentration has resulted to increase in adsorption capacity. The maximum dye adsorption capacity corresponding to 1.6 mg/g was reached at 50 mg/L. The increase in the initial dye concentrations resulted to an increase in the number of molecules present in the solution thereby surrounding more of the active sites and this promotes an interaction between the dye molecule and the solid surface adsorbent thereby causing increase in adsorption capacity [19]. However, after attaining

the equilibrium concentration, there was a decrease in adsorption capacity due to the saturation of the active sites on the adsorbent surface. A similar observation has been reported [20].

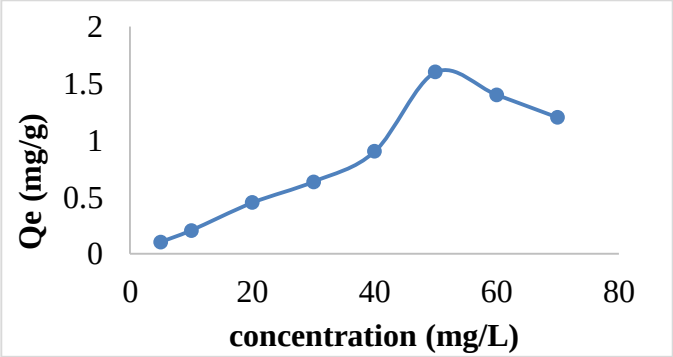

Fig. 4: Effect of initial concentration on adsorption of Rhodamine B onto CuO/CA nanocomposite

Effect of contact time

The influences of contact time on adsorption of dye onto CuO/CA nanocomposite adsorbent (Fig. 5) strongly affect the adsorption capacity. It was observed that the adsorption capacity increases with increase in contact time as a result of vacant adsorption sites that are available for the electrostatic interaction with the dye molecules, but after attaining the equilibrium time (180 minutes), no further increase in adsorption capacity was noticed. This could be attributed to the lack of available adsorption site for uptake of dye molecule [21]. The maximum adsorption capacity obtained at optimum time was 41.68 mg/g.

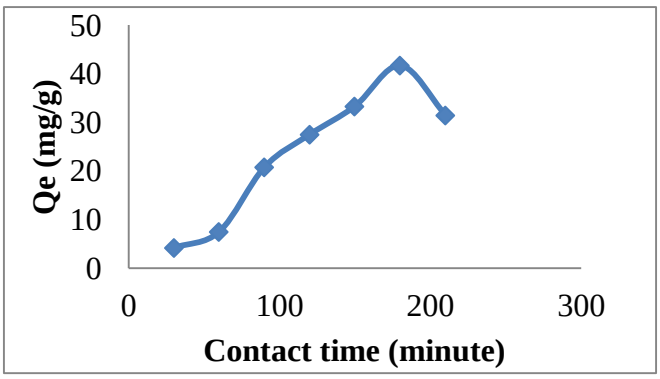

Fig. 5: Effect of contact time on adsorption of Rhodamine B onto CuO/CA nanocomposite

Effect of adsorbent dosage

The effect of adsorbent dosage on adsorption of Rhodamine B dye onto CuO/CA nanocomposite is shown in Fig 6. The maximum adsorption capacity achieved was 2.34 mg/g using optimum adsorbent dosage of 0.1 g. It could be observed that increase in adsorbent dosage resulted to decrease in adsorption capacity. This could be attributed to the aggregation or overlapping of the various adsorption sites thereby causing a decrease in total surface area and subsequently lower the adsorption capacity. A similar observation has been reported in literature [22].

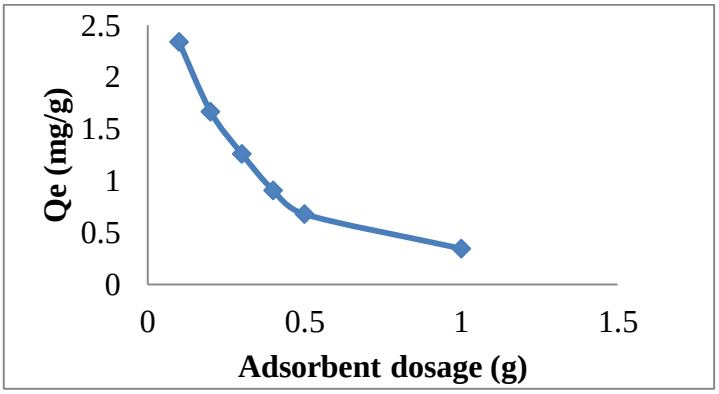

Fig. 6: Effect of adsorbent dosage on adsorption of Rhodamine B onto CuO/CA nanocomposite

Effect of Temperature

Temperature profile diagram for the uptake of dye onto CuO/CA nanocomposite is shown in Fig. 7. It was observed that increase in temperature resulted to increase in adsorption indicating an endothermic process. The maximum adsorption capacity achieved at 434 K corresponds to 9.51 mg/g. This observation is related to the increase in mobility of the dye molecules at higher temperatures which leads to increase in collision and binding of the dye molecules with the adsorption sites [21].

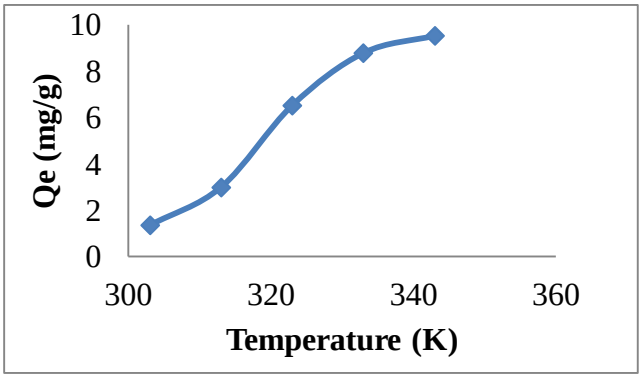

Fig. 7: Effect of temperature on adsorption of dye onto CuO/CA nanocomposite

Adsorption Isotherm

Langmuir Isotherm

This isotherm is based on assumptions that the adsorption takes place in the form monolayer in which only molecule of the adsorbate can be attached to the surface of the adsorbent [23]. The general equation of Langmuir isotherm is given by Eq. 2:

$$\frac{C_e}{q_e} = \frac{1}{K_L q_m} + \frac{C_e}{q_m} \qquad (2)$$

Where Ce is the equilibrium concentration (mg/L), qe is the amount of adsorbent adsorbed at equilibrium (mg/g), q_m is the maximum adsorption capacity to complete monolayer coverage on adsorbent surface (mg/g) and K_L is the Langmuir constant related to the energy of adsorption (L/mg). Plotting a graph of $\frac{C_e}{q_e}$ against C_e, gives a straight line graph (Fig. 8) with slope $\frac{1}{q_m}$ and intercept $\frac{1}{K_L q_m}$

The value of separation factor (R_L), Eq. (3) is very useful in determining wether the adsorption process is favorable or not.

$$R_L = \frac{1}{1 + K_L C_0} \qquad (3)$$

Where R_L is the separation factor, C_o is the initial concentration (mg/L)

When R_L value is greater than 1 it indicates unfavorable adsorption, R_L value equal to 1, the adsorption is linear. When R_L value is between 0 and 1, the adsorption is favorable and if R_L value is equal to 0, the adsorption is irreversible [17].

Freundlich Isotherm

Freundlich adsorption model assumes that the adsorbents have a heterogeneous surface with different adsorption capacity [24]. The linearized form of Freundlich model can be expressed by Eq. (4):

$$\log q_e = \log K_F + \frac{1}{n} \log C_e \qquad (4)$$

Where Ce is the equilibrium concentration of the adsorbate (mg/L), qe is the amount of adsorbate adsorbed per unit mass of adsorbent (mg/g), K_F (mg/g(L/mg)$^{1/nF}$) and n (L/mg) are Freundlich

constants representing the adsorption capacity and intensity of adsorption respectively. Plotting a graph of log qe against log Ce, gives a straight line graph with slope $\frac{1}{n}$ and the intercept Log K_F (Fig. 9). When the value of n lies between 1 and 10 it indicates a favorable adsorption process and if the value of 1/n is below 1, it indicates a favourable normal adsorption at low concentration while if the value of 1/n is above 1 it indicates cooperative adsorption or unfavourable adsorption [15].

It could be observed from Table 2 that the R_L value was 0.09 indicating a favourable adsorption process. The maximum value of Langmuir monolayer coverage (q_m) and Langmuir isotherm constant, K_L were 0.60 mg/g and 0.186 L/mg respectively. The value of correlation coefficients, R^2 was 0.920 which indicates the equilibrium data fitted well with Langmuir isotherm model. It was also observed from the Freundlich constants (Table 2) that the R^2 value (0.793) was lower than that of Langmuir model, thus indicating poor fitting while the value of 1/n (0.534) fell below 1 and this indicates normal and favourable adsorption process whereas K_F was found to be 0.110 mg/g(L/mg)$^{1/nF}$

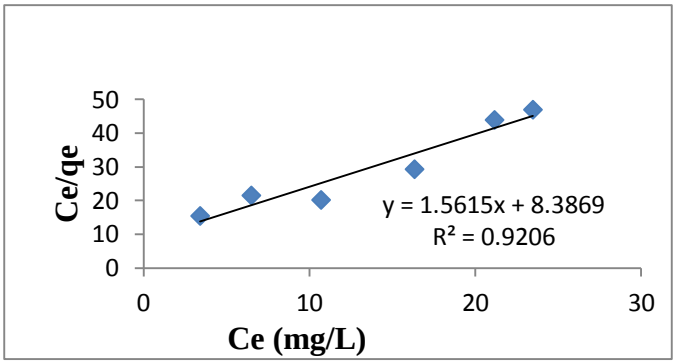

Fig. 8: Langmuir plot of Rhodamine B dye adsorption onto CuO/CA composite

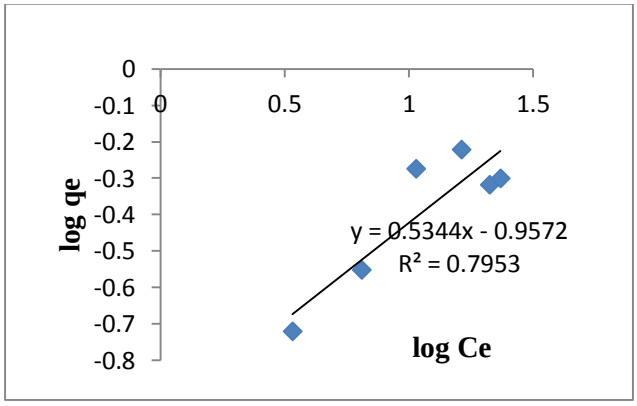

Fig. 9: Freundlich plot of Rhodamine B dye adsorption onto CuO/CA composite

Table 2: Isotherm parameters of Rhodamine B dye adsorption onto CuO/CA composite

Adsorbent		Langmuir			Freundlich		
	q_m (mg/g)	K_L (L/mg)	R_L	R^2	K_F (mg/g(L/mg)$^{1/nF}$)	1/n (L/mg)	R^2
CuO-CA	0.640	0.186	0.09	0.920	0.110	0.534	0.795

Adsorption Kinetics

Pseudo first-order kinetic

The general form of pseudo first-order equation can be expressed by Eq. 5:

$$\log(q_e - q_t) = \log q_e - \frac{k_1}{2.303} t \qquad (5)$$

Where k_1 is the equilibrium rate constant for pseudo-first-order model (min^{-1}), q_e and q_t represents the amounts of metal ions adsorbed per gram of adsorbent (mg/g) at equilibrium and at time t (min), respectively [25]. A plot of $\log(qe - qt)$ versus time, t (min) gives a straight line graph (Fig. 10) from which the values of k_1 and q_e can be determined from the slope and intercept respectively.

Pseudo second-order kinetic

The general form of pseudo second-order equation is given by Eq. 6:

$$\frac{t}{q_t} = \frac{1}{k_2 q_e^{\,2}} + \frac{1}{q_e} t \qquad (6)$$

Where k_2 is the pseudo second-order rate constant (g/mg/min), q_e and q_t are the amounts of metal ions adsorbed per gram of adsorbent (mg/g) at equilibrium and at time t (min) respectively. A plot of t/qt against t gave a straight line graph (Fig. 11). The values of q_e and k_2 can be obtain from the slope and intercept respectively [26].

It could be observed from Table 3 that the R^2 value obtained from pseudo first-order was low (0.556) which shows poor fitting while the R^2 value of pseudo second-order was high (0.968) which indicates the applicability of this model compared to pseudo first-order model. However, the values of Qe calculated from pseudo first-order was by far lower than the value

experimentally Qe whereas the corresponding values obtained from pseudo second-order were in good agreement with each other. This also showed the kinetic data of the adsorption system was well described by pseudo second-order model. This is based on the assumption that the rate limiting step is chemisorptions involving valence forces by sharing or exchange of electrons between the adsorbate and adsorbent [27].

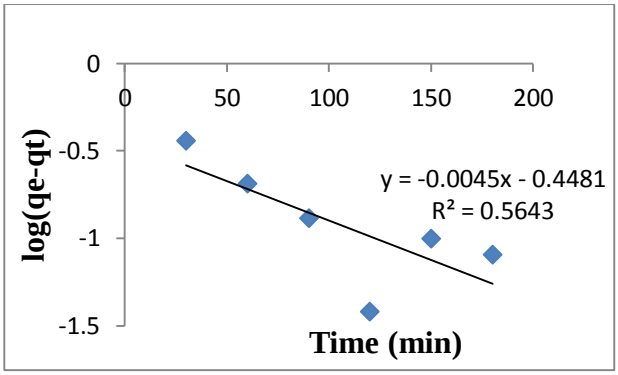

Fig. 10: Pseudo first-order plot of Rhodamine B dye adsorption onto CuO/CA composite

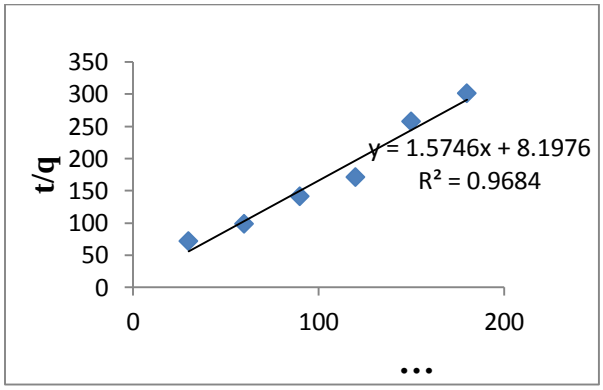

Fig. 11: Pseudo second-order plot of Rhodamine B dye adsorption onto CuO/CA composite

Table 3: Kinetic parameters of Rhodamine B dye adsorption onto CuO-CA composite

Kinetic model	Parameter	Value
Pseudo first-order	Qe Cal. (mg/g)	0.314
	Qe Exp.(mg/g)	0.803
	k_1 (min^{-1})	0.09
	R^2	0.564
Pseudo second-order	Qe Cal. (mg/g)	0.781
	Qe Exp.(mg/g)	0.803
	k_2 (g/mg min^{-1})	0.302
	R^2	0.968

Adsorption Thermodynamics

Thermodynamic parameters such as change in Gibbs free energy (ΔG) enthalpy change (ΔH), and entropy change (ΔS) were calculated using Eqs. (13), (14) and (15) respectively. The values of thermodynamic parameters are presented in Table 4.

$$\Delta G = - RT \ln Kc \quad (7)$$

$$\ln Kc = \frac{\Delta S}{R} - \frac{\Delta H}{RT} \quad (8)$$

$$\Delta G = \Delta H - T\Delta G \quad (9)$$

Where T is the absolute temperature (K), R is the ideal gas constant (8.314 J/mol/K), Kc is the distribution coefficient. The values for ΔH and ΔS can be determined from the slopes and intercepts of the Van't Hoff plot (Fig. 12) of *ln Kc* versus 1/T [28].

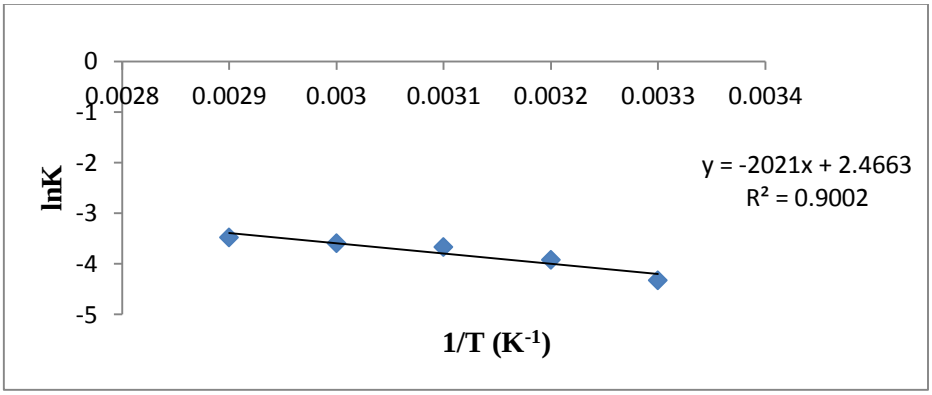

Fig. 12: Thermodynamic plot of Rhodamine B dye adsorption onto CuO/CA composite

Table 4: Thermodynamic parameters of Rhodamine B dye adsorption onto CuO/CA composite

Adsorbent	Temperature (K)	ΔG (kJ/mol)	ΔH (kJ/mol)	ΔS (J/mol/K)	R^2
CuO/CA	303	- 6.19	11.80	9.50	0.990
	313	- 6.40			
	323	- 6.61			
	333	- 6.81			
	343	-7.02			

The values of thermodynamic parameters are presented in Table 4. It could be observed that the values of Gibb's free energy ΔG, were negative as the temperature increased from 303 to 343 K which is an indication that the adsorption of Rhodamine B dye onto CuO/CA composite was feasible and spontaneous in nature. The positive values of enthalpy change (11.80 kJ/mol) and entropy change (9.50 J/mol/K) revealed endothermic process and increased in randomness at solid-solution interface respectively. A similar observation has been reported in the literature [10].

CONCLUSION

Adsorbent derived from copper(II) oxide and cellulose acetate, CuO/CA has been used for the removal of Rhodamine B from aqueous solution. The result of batch adsorption experiments showed that the uptake of dye onto CuO/CA composite was affected by initial concentration of the adsorbate, contact time, adsorbent dose and temperature. The study demonstrated that adsorbents produced from low cost agricultural based materials could be used effectively to remove Rhodamine B dye from aqueous solution. Adsorption isotherms and kinetic studies were best described by Langmuir isotherm model and pseudo second-order kinetic model respectively while the value of thermodynamic parameters revealed feasible, spontaneous and endothermic process with increase in randomness at the interface.

REFERENCES

[1] Nigam, P., Armour, G., Banat, I. M., Shengli, D. & Marchant, R. (2000). Physical removal of textile dyes from effluents and solid-state fermentation of dye-adsorbed agricultural residues. *Bioresource Technology*, 72(3), 219–226.

[2] Tarapitakcheevin, P., Weerayutsil, P. & Khuanmar, K. (2013). Adsorption of acid dye on activated carbon prepared from water hyacinth by sodium chloride activation. *GMSARN International Journal*, *7*, 83-90.

[3] Kadirvelu, K., Thamaraiselvi, K. & Namasivayam, C. (2016). Removal of heavy metals from industrial wastewaters by adsorption onto activated carbon prepared from an agricultural solid waste. *Bioresource Technology*, *76*(1), 63-65.

[4] Gogate, P.R. & Pandit, A.B. (2004). A review of imperative technologies for wastewater treatment I: oxidation technologies at ambient conditions. *Advances in Environmental Research*, *8*(3-4), 501-551.

[5] Abdullahi, M. R. & Nwosu, F. O. (2022). Equilibrium and kinetic studies on the removal of mordant black 11 dye from aqueous solution and real tannery effluents using $CuFe_2O_4$/Ac nanocomposites, *Applied Journal of Environmental Engineering Science*. 8(4), 286-299.

[6] Dada, A.O., Olalekan, A.P., Olatunya, A.M. & Dada, O. (2012). Langmuir, Freundlich, Temkin and Dubinin–Radushkevich Isotherms Studies of Equilibrium Sorption of Zn^{2+} Unto Phosphoric Acid Modified Rice Husk. *IOSR Journal of Applied Chemistry*. 3(1), *38-45*.

[7] Pinto, R. J. B., Neves, M.C., Neto, C.P. & Trindade, T. (2012). Composites of cellulose and metal nanoparticles. *Nanocomposites–New Trends and Developments*, 1-25.

[8] Kamaraj, M., Srinivasan, N.R., Aseefa, G., Adugna, A.T. & Kebede, M. (2020). Facile development of sunlit ZnO nanoparticles-activated carbon hybrid from pernicious weed as an operative nano adsorbent for removal of methylene blue and chromium from aqueous solution: Extended application in tannery industrial waste water. *Environmental Technology and Innovation*, 17, 100540.

[9] Alorabi, A. Q., Hassan, M.S. & Azizi, M. (2020). Fe_3O_4-CuO-activated carbon composite as an efficient adsorbent for bromophenol blue dye removal from aqueous solutions. *Arabian Journal of Chemistry*, 13, 8080–8091.

[10] Inyinbor, A.A., Adekola, F.A. & Olatunji, G.A. (2016). Kinetics, isotherms and thermodynamic modeling of liquid phase adsorption of Rhodamine B dye onto Raphia hookerie fruit epicarp. *Water Resources and Industry* 15, 14–27.

[11] Rahdar, A., Aliahmad, M., & Azizi, Y. (2015). NiO Nanoparticles: Synthesis and Characterization, *Journal of Nanostructures*, 5, 145- 151.

[12] Tahir, P.M., Zaini, L.H., Jonoobi, M. & Khalil, H.A. (2015). Preparation of Nanocellulose from Kenaf (Hibiscus cannabinus L.) via Chemical and Chemo-mechanical Processes. *Handbook of Polymer Nanocomposites. Processing, Performance and Application*: Polymer *Nanocomposites of Cellulose Nanoparticles*, 119-144

[13] Adebayo, G.B., Jamiu, W., Okoro, H.K., Okeola, F.O., Adesina, A.K. & Feyisetan, O.A. (2019). Kinetics, Thermodynamics and Isothermal Modelling of Liquid Phase Adsorption of Methylene Blue onto Moringa Pod Husk Activated Carbon. *South African Journal of Chemistry*, *72*, 263-237.

[14] Karabelli, D., Ünal, S., Shahwan, T. & Eroğlu, A.E. (2011). Preparation and characterization of alumina-supported iron nanoparticles and its application for the removal of aqueous Cu^{2+} ions. *Chemical Engineering Journal*, *168*(2), 979-984.

[15] Adegoke, H.I., Adebayo, G.B. & Fauzeeyat, S. (2020). Adsorption of Cr (VI) ions onto goethite, activated carbon and their composite: kinetic and thermodynamic studies. *Applied Water Science*, 10 (9), 1-18.

[16] Jain, M., Yadav, M., Kohout,T., Lahtinen, M., Garg, V. K. & Sillanpaa, M. (2018). Development of iron oxide/activated carbon nanoparticle composite for the removal of Cr(VI), Cu(II) and Cd(II) ions from aqueous solution. *Water Resources and Industry* 20, 54–74.

[17] Williams, P.T. & Reed, A. R. (2006). Development of activated carbon pore structure via physical and chemical activation of biomass fibre waste. *Biomass Bioenergy*, 30, 144–152.

[18] Akpomie, K.G. & Dawodu, F.A. (2015). Potential of a low-cost bentonite for heavy metal abstraction from binary component system. *Journal of Basic Applied Sci*ences, 4, 1-13.

[19] Han, X., Niu, X. & Ma, X. (2012). Adsorption characteristics of methylene blue on poplar leaf in batch mode: Equilibrium, kinetics and thermodynamics. *Korean Journal of Chemical Eng*ineering, 29(4), 494-502.

[20] Khasri, A., Jamir, M.R.M., Ahmad, A. A. & Ahmad M.A. (2021). Adsorption of Remazol brilliant violet 5R dye from aqueous solution onto melunak and rubber wood sawdust based activated carbon: interaction mechanism, isotherm, kinetics and thermodynamic properties. *Desalination and Water Treatment*. 216, 401-411.

[21] Wong, S., Abd Ghafar, N. Ngadi, N., Razmi, F. A. Inuwa, I.M., Mat, R. & Amin, N. A. S. (2020). Effective removal of anionic textile dye using adsorbent synthesized from coffee waste. S*cientific Reports*, 10 (1), 1-13.

[22] Shukla, A., Dorris, K.L. & Zhang, Y. (2000). The Removal of Heavy Metal from Aqueous Solutions by Sawdust Adsorption-Removal of Copper. *Journal of Hazardous Materials*, 80 (1 – 3), 33-42.

[23] Langmuir I. (1918). The adsorption of gases in plane surfaces of glass, mica and platinum. *Journal of American Chemical Society*, 40, 1361-1403.

[24] Freundlich, H.M.F. (1906). Over the adsorption in solution. *Journal of Physical Chemistry*, *57*, 385–471.

[25] Lagergren, S. (1898). About the theory of so-called adsorption of soluble substance, *Kungliga SvenskaVetenskapsakademiens Handlinger*, 24 (4), 1-39.

[26] Ho, Y. S. & Mckay, G. (1999). Pseudo second-order model for sorption processes. *Process Biochemistry*, 34, 451 – 465.

[27] Pathania, D., Sharma, S. & Singh, P. (2017). Removal of methylene blue by adsorption onto ficus carica bast. *Arabian Journal of chemistry*, 10, 1445- 1451.

[28] Adebayo, G. B., Adegoke, H.I., Jamiu, W., Balogun, B.B. & Jimoh, A.A. (2015). Adsorption of Mn(II) and Co(II) ions from aqueous solution using Maize cob activated carbon: Kinetics and Thermodynamics Studies. *Journal of Applied Science and Environmental Management*, 19 (4), 737- 748.